CrossMark

ORIGINAL ARTICLE

Investigating the characteristics of mine water in a subsea mine using groundwater geochemistry and stable isotopes

Fengshan Ma[1] · Haijun Zhao[1] · Jie Guo[1]

© Springer-Verlag Berlin Heidelberg 2015

Abstract Investigation were conducted in the Xinli subsea mine from 2006 to 2011, which is the largest subsea mine in China and threatened by the overlying Quaternary aquifer and seawater. Hydrochemical and stable isotopic (δ^2H and δ^{18}O) analyses were used to study the relationships between various waters. Hydrochemical results indicated that the seepage water in the mine tunnels had higher EC, TDS, and concentrations of most elements than the seawater and saline groundwater. Water analyses indicated the mine discharge was a mixture of the seawater, brine, and atmospheric precipitation. The proportions of the three different sources were calculated based on hydrochemical and isotopic analyses. The seepage water were more isotopically enriched than the seawater but less than the brine. In addition, the isotope mixing calculation indicated that the average proportions of mine water from seawater, brine and atmospheric precipitation were about 38.5, 46, and 15.5 % respectively for the entire mine in 2006. However, the concentrations of these analyses decreased and the proportion of the seawater increased 21.1 % after 5 years of exploitation in 2011. These changes demonstrated that the surrounding rock mass underwent a certain extent of deformation and failure because of the mining disturbance, which enhanced the permeability of the surrounding rock mass.

✉ Haijun Zhao
zhaohaijun@mail.iggcas.ac.cn

[1] Key Laboratory of Shale Gas and Geoengineering, Institute of Geology and Geophysics, Chinese Academy of Sciences, Beijing 100029, China

Introduction

Mining exploitation under the seawater is becoming a promising industry for resource development (Ghosh and Mukhopadhyay 2000). Until now, several countries have already carried out mining engineering under the sea area, including Britain, Australia, Turkey, Chile, Japan, Canada, China and so on (Glasby 2002; Li et al. 2013; Sui and Xu 2013; Wang et al. 2013). In these countries, subsea mining activities were managed strictly by the government regulations and the mining technology were developed slowly because of the complex mining conditions and serious issues on mining safety (Castilla and Nealler 1978; Aston and Whittaker 1985; Jewett et al. 1999; Glasby 2000). The potential water bursting disaster is undoubtedly one of the most concerned issues for subsea mining (Garritty 1983; Halfar and Fujita 2002; Sui and Xu 2013). The hydraulic connection between the seawater and mine water has always been the focus of the study (Garritty 1983; Aston and Whittaker 1985; Wang et al. 2013). The implementation of successful hydraulic remedies or engineering treatment schemes depends largely on identifying sources of groundwater to the mine tunnels (Li et al. 2013).

Geochemistry and stable isotope characteristics have been widely used to study interactive relationship between water from different origins (Pellicori et al. 2005; Migaszewski et al. 2009; Mahmoud et al. 2013). In general, isotopic compositions of water are changeless over a short period. Therefore, a large number of researches have demonstrated successful applications of geochemistry and isotopic data on origin assessment of mining environments (Katherine and Eileen 2009; Chapman et al. 2013), groundwater contamination (Parker et al. 2012; Gammons et al. 2013), hydrothermal alteration (Birkle et al. 2001; González-Partida et al. 2005), and seawater intrusion in

coastal environment (Park et al. 2012; Garing et al. 2013). In general, the geochemistry and isotopic features of seawater, brine, freshwater, and their mixtures are different because of their different origins (Ma et al. 2007; Han et al. 2011). Sampling and testing flowing water's chemical properties at locations where groundwater entered the mine tunnel could enable assessment of water origins that contributed to the mine water in tunnels (Katherine and Eileen 2009). Therefore, geochemistry and stable isotopic analysis could potentially be used in understanding and investigating the sources and characteristics of water associated with subsea mining mine.

This paper presents a study from a subsea gold mine in Shandong province, China. The management of this mine requires an understanding of the mine discharge characteristics. A number of water samples which contained seawater, brine, freshwater, and seepage water were sampled and measured in July of 2006 and July of 2011, giving additional insight into the hydrogeological features and processes at the mine tunnels. Based on the extensive data set, this research mainly aims to demonstrate how major ion chemistry and isotopes analyses can be combined in the subsea mine to (i) estimate the contribution of water sources to the mine discharge, (ii) quantify the variations of seepage discharge, and (iii) improve the understanding of the mining impact on rock mass permeability.

Study area and background

The Xinli gold mine is located in the Laizhou Bay, eastern China. Currently, it is the largest subsea mining mine in China because of its vast gold reserves at the bottom of the Bohai Sea (Figs. 1, 2) (Sun et al. 2002). The Xinli region is board and flat with low elevation in the coastal zone (1.2–4.5 m). In the study area, the Bohai Sea serves as the local base level of erosion. The Wang River is distributed on the east side of the mine, which is the only surface runoff within the mine area. The vast majority of the western and northern areas are covered by seawater. The Quaternary sediments are distributed throughout the shallow portion of the ground with an outcrop at the SE part, with a varying thickness of 16–46 m sandy clay, fine sand, medium coarse sand, and coarse gravel with diverse sedimentary sequence and poor regularity. The Xinli area is sub-humid warm temperate continental monsoon climate. The mean annual temperature and precipitation are 12.5 °C and 597.8 mm, respectively.

The mine is characterized by the Sanshandao–Cangshan fault, which is the ore-controlling structure (Figs. 1, 2). This fault is partially outcropped to the surface. The exposed part is about 12 km long and 50–200 m wide and displays an S-shaped distribution. The fault is oriented N62°E in the west and other coordinate to N38°E. It has an average dip angle of 46° and extends more than 600 m deep. Furthermore, it has compressed shearing mechanical properties and is marked by impermeable fault gouges in the fault plane. According to the exposure data on drillings and mining (Sun et al. 2002), the fault gouge varies from 0.05 to 0.1 m and shows extremely low permeability. Thus, it can be served as a good water-resistant layer that separates the hydraulic connection between the hanging wall rock mass and the footwall rock mass. The mineralized zone of the fault is about 1300 m long, 70–185 m wide, and extends from about −40 m to below level −1000 m under the sea level. The strike of the deposit is N60°–70°E, dipping SE at an angle of 40°–50° (Sun et al. 2002).

The seawater above the mine is a key issue for subsea mining. For the sake of safety, different functional mine shafts and upward cut-and-fill mining method has been adopted from −165 m sublevel to −400 m sublevel of the mine. The height of one mining level is 40 m. But so far the −105 and −135 m sublevels are unexploited for security reasons because they are close to the bottom of the Bohai Sea. The distance between two barrier pillars is 100 m and the side length of the square panel pillar is 5 m. In the respect of mining design, the mining sequence is from bottom to top by excavating and filling at a slice height of 2 m. During the mining process, tens of access drifts are arranged in every delamination layer to increase the mineral production.

The overlying Quaternary sediments are characterized by porous water-bearing structure and have direct hydraulic connection with the seawater. Fortunately, a layer of silt soil and mild clay was deposited along the contact zone between the bottom of the Quaternary sediments and the upper interface of the bedrock. This layer is about 1–10 m thick and nearly impermeable to inhibit the seawater from infiltrating the seabed rock mass. However, the cohesion strength of the clay is very low and it can hardly bear any tension stress if ground subsidence is induced by mining activity (Li et al. 2013).

In addition, the Quaternary sediments are underlain by magmatic and metamorphic rocks (Sun et al. 2002). These rocks are mainly composed of medium-to fine-grained metagabbro, monzonitic granite, beresitization granite, and beresitization cataclasite, and permeability is related to the different embedded depths and locations. Generally, joints and original structural planes are well developed in the shallow position because of natural weathering. The degree of fractural development is relatively higher in the hanging wall bedrock than that in footwall bedrock. The fissured bedrock aquifer has poor natural circulation conditions, and is mainly recharged through the leakage of the upper Quaternary aquifer system. Therefore, the geological backgrounds and mining environments shows that the Xinli
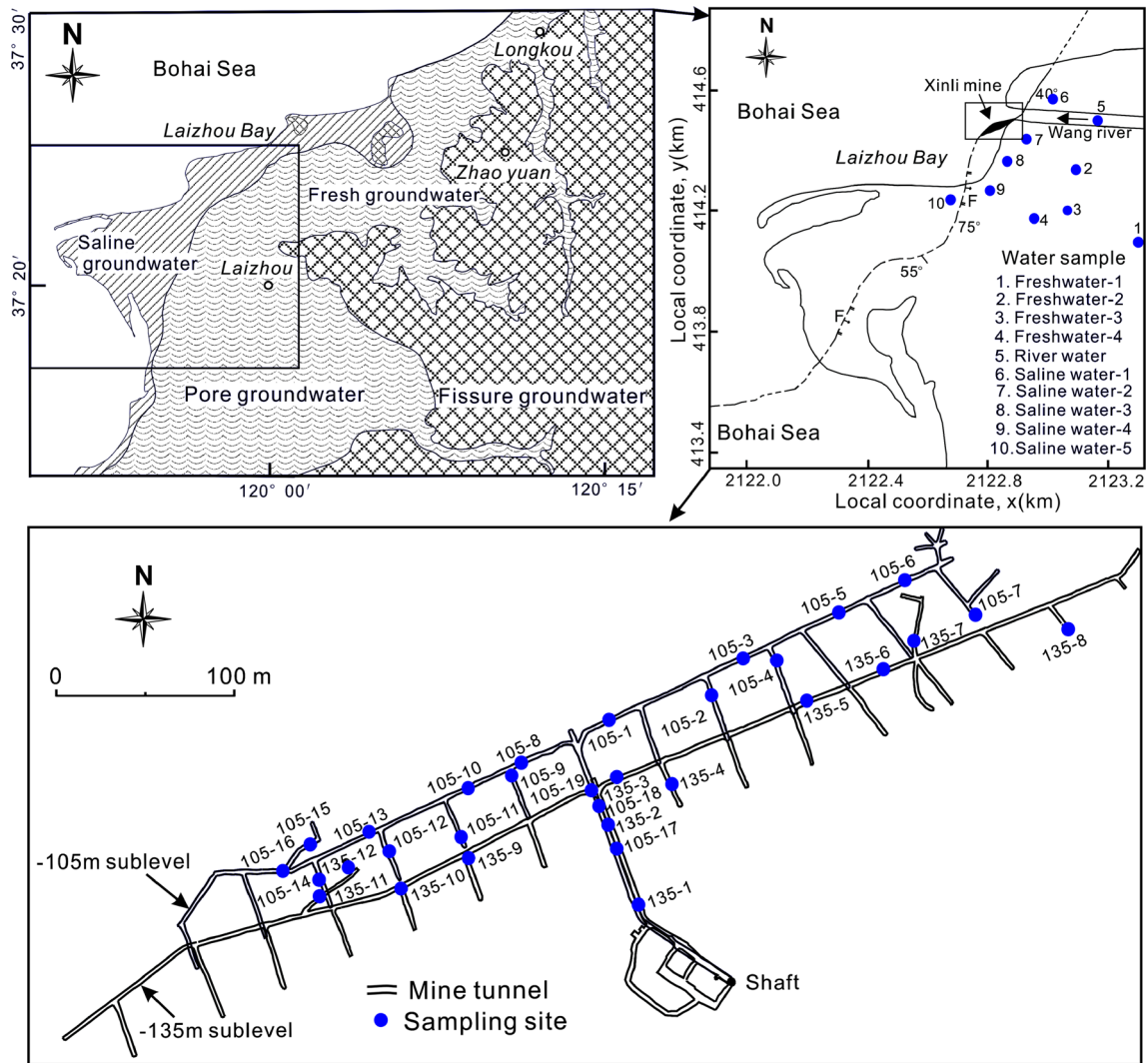
Fig. 1 Study area of Xinli mine, showing location of water samples (*solid circles*). Sample numbers correspond to Tables 1 and 2

gold mine is under threat from seawater gushing. A large number of water seepage sites have occurred in the mine tunnels after several years of mining. Therefore, it is very important to understand the origins and mechanisms of water gushing so as to propose a proper plan of prevention and management of water bursting disaster.

Sampling and measurements

From 2006 through 2011, two-phase fieldwork was performed in the Xinli mine area. In July 2006, a total of 43 water samples were collected in the mine tunnels and peripheral areas of the mine for chemical analyses. These samples include 19 seepage water samples from the −105 m sublevel of the mine tunnels, 12 seepage water samples from the −135 m sublevel of the mine tunnels, 5 saline groundwater samples from wells at the Quaternary

water-rich phreatic aquifer, 4 freshwater samples from wells at the upper reaches of the Wanghe River, 2 seawater samples from the Bohai Sea and 1 surface water from the Wanghe River to assess the potential contribution of mine discharge (Table 1). To further study the variations in chemical components of the seepage water and estimate the mining impact on the permeability of surrounding rock, the same determinations were also performed on 18 seepage water samples in July 2011, i.e., 10 seepage water samples from the −105 m sublevel of the mine tunnels, and 8 seepage water samples from the −135 m sublevel of the mine tunnels (Table 2). It is worth emphasizing that the second round sampling sites were the same as those in the first round of sampling.

Field parameters including pH, specific conductivity (EC), and temperature (T) of the water samples were measured in situ by portable digital pH measuring apparatus, conductivity measuring apparatus, and thermometer.
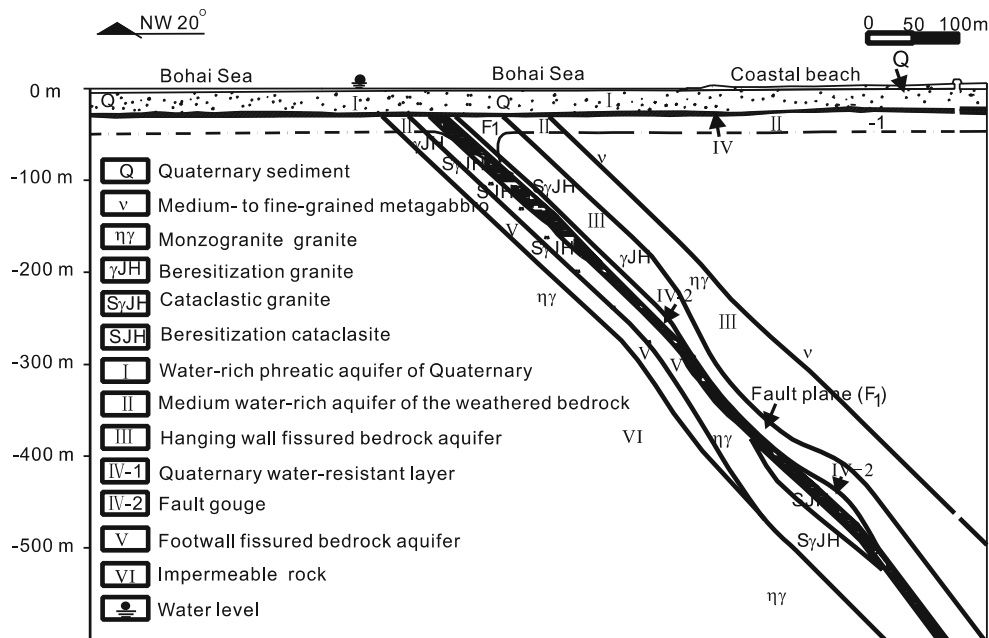
Fig. 2 Geological cross-section of Xinli mine

All water samples were filtered with common filters (0.2 μm) to remove insoluble solids for chemical analysis. The water samples were preserved at 5 °C in plastic bottles with air-tight seals prior to analysis. The chemical analyses were performed in the Institute of Geology, China Earthquake Administration. All water samples were analyzed based on the test method and the standards of People's Republic of China (GB7477-87, GB7476-87, GB11899-89, and GB11904-89). The analyzed chemical species included sodium (Na^+), calcium (Ca^{2+}), magnesium (Mg^{2+}), potassium (K^+), chloride (Cl^-), sulfate (SO_4^{2-}), bicarbonate (HCO_3^-) in milligram per liter (mg/L). Besides, the total dissolved solids (TDS), alkalinity and total hardness were also measured.

Stable isotope analysis of the seepage water samples were performed at the Laboratory for Stable Isotope Geochemistry, Institute of Geology and Geophysics, Chinese Academy of Sciences. Hydrogen-isotope-ratio analysis utilized a hydrogen equilibration technique (Révész and Coplen 2007). Oxygen-isotope-ratio analysis utilized a H_2O–CO_2 equilibrium technique (Epstein and Mayeda 1953; Révész and Coplen 2008). The ratio of the heavy isotopes of oxygen and hydrogen to that of the lighter isotopes is represented by the abundance ratio "R". The isotopic composition is represented by delta (δ), which is the deviation of "R" from that of a reference material (VSMOW):

$$\delta^{18}O_{sample} = \left(\frac{(^{18}O/^{16}O)_{sample}}{(^{18}O/^{16}O)_{reference}} - 1 \right) \times 1000, \qquad (1)$$

$$\delta^{18}H_{sample} = \left(\frac{(^{18}H/^{16}H)_{sample}}{(^{18}H/^{16}H)_{reference}} - 1 \right) \times 1000, \qquad (2)$$

where $\delta^{18}O_{sample}$ and $\delta^{18}H_{sample}$ are the results, in ‰; $^{18}O/^{16}O_{sample}$ and $^{18}H/^{16}H_{sample}$ are the O and H isotope ratios in the water samples and $^{18}O/^{16}O_{reference}$ and $^{18}H/^{16}H_{reference}$ are the O and H isotope ratios in the reference samples. The analytical precisions of the stable isotopes were within the two-sigma uncertainties of the analytical methods of 0.2 ‰ for O and 2 ‰ for H.

Results

Water geochemistry

Filed parameters (pH, TDS, and temperature), anion concentrations (Cl^-, SO_4^{2-}, HCO_3^-), and major cation concentration for the water samples are reported in Table 1 (July 2006). The first round of seepage water samples had near-neutral pH (Avg. 7.12, SD 0.28), prominent EC (Avg. 7.04×10^4 μS cm^{-1}, SD 1.31×10^4), high Cl^- (Avg. 3.03×10^4 mg L^{-1}, SD 7.32×10^3 mg L^{-1}), Na^+ concentration (Avg. 16.4×10^4 mg L^{-1}, SD 3.79×10^4 mg L^{-1}), and TDS (Avg. 5.41×10^4 mg L^{-1}, SD 1.28×10^4 mg L^{-1}).

In contrast to the −105 m sublevel, the seepage water sampled in the deeper −135 m sublevel showed higher TDS, EC, and concentrations of most of cations and anions. However, the mean pH was 6.95 (SD 0.32) in the −135 m sublevel versus 7.23 (SD 0.2) in the −105 m sublevel.

Table 1 Chemical composition of water samples collected in July 2006

Sample	pH	EC (μS/cm) × 10^4	TDS (mg/L) × 10^4	Cl$^-$ (mg/L) × 10^4	SO$_4^{2-}$ (mg/L) × 10^3	HCO$_3^-$ (mg/L) × 10^2
105-1	6.92	5.69	3.72	2.06	2.71	2.68
105-2	7.02	5.86	4.17	2.32	3.10	2.95
105-3	7.16	5.84	4.10	2.26	3.00	2.44
105-4	7.16	6.23	4.38	2.47	2.98	2.38
105-5	7.33	5.42	3.86	2.14	2.93	2.62
105-6	7.40	5.59	4.35	2.40	3.12	2.44
105-7	7.15	8.18	6.87	3.91	4.42	2.68
105-8	7.56	5.04	3.81	2.11	2.88	2.75
105-9	7.46	5.14	3.91	2.16	2.83	2.87
105-10	7.42	5.78	4.41	2.44	3.31	2.68
105-11	7.40	6.38	5.04	2.78	3.36	3.17
105-12	7.34	7.20	5.91	3.29	4.13	3.23
105-13	7.31	7.72	6.40	3.60	4.51	3.30
105-14	7.40	8.05	6.80	3.81	4.68	3.36
105-15	6.95	7.33	6.08	3.40	4.16	2.68
105-16	6.88	9.32	8.26	4.63	5.28	2.81
105-17	7.08	6.62	5.22	2.98	3.00	2.07
105-18	7.14	8.43	7.06	3.96	4.76	2.81
105-19	7.30	7.06	5.65	3.14	3.96	2.75
135-1	6.74	7.86	5.78	3.33	3.27	2.20
135-2	6.91	7.96	5.81	3.32	3.75	2.87
135-3	6.43	7.12	5.15	2.87	3.69	2.50
135-4	6.72	6.49	4.58	2.62	3.07	1.95
135-5	7.09	5.99	4.17	2.35	2.88	2.50
135-6	7.21	6.01	4.16	2.35	2.88	2.44
135-7	7.23	6.18	4.25	2.39	3.04	2.50
135-8	7.09	9.80	7.68	4.36	4.96	2.50
135-9	7.20	8.40	6.29	3.54	4.17	2.26
135-10	7.23	8.21	6.10	3.42	4.27	2.68
135-11	7.20	8.73	6.62	3.71	4.51	3.23
135-12	6.37	8.81	6.97	3.91	4.92	2.75
Seawater-1	7.59	4.44	3.00	1.65	2.44	1.59
Seawater-2	7.66	4.42	2.94	1.63	2.27	1.53
Saline water-1	7.08	5.22	3.84	2.06	2.88	3.17
Saline water-2	7.18	4.95	3.53	1.98	2.47	2.26
Saline water-3	7.29	4.15	2.81	1.52	2.40	1.83
Saline water-4	7.23	4.41	3.07	1.69	2.21	2.07
Saline water-5	7.28	4.61	3.14	1.75	2.23	1.77
Freshwater-1	7.37	0.08	0.06	0.01	0.08	1.40
Freshwater-2	7.42	0.18	0.13	0.02	0.41	2.56
Freshwater-3	7.27	0.35	0.22	0.08	0.33	2.14
Freshwater-4	7.67	0.06	0.04	0	0.06	2.10
River water	7.08	0.15	0.10	0.03	0.13	2.20

Sample	Ca^{2+} (mg/L) × 10^3	Mg^{2+} (mg/L) × 10^3	Na$^+$ (mg/L) × 10^4	K$^+$ (mg/L) × 10^2	δ^{18}O (‰)	δ^{2}H (‰)
105-1	0.72	1.18	1.15	2.08	−1.8	−25.4
105-2	0.65	1.43	1.28	2.13	−2.2	−27.6

Table 1 continued

Sample	Ca^{2+} (mg/L) $\times 10^3$	Mg^{2+} (mg/L) $\times 10^3$	Na^+ (mg/L) $\times 10^4$	K^+ (mg/L) $\times 10^2$	$\delta^{18}O$ (‰)	δ^2H (‰)
105-3	0.68	1.41	1.28	2.13	−2.3	−28.4
105-4	0.88	1.58	1.33	1.93	−2.8	−31.4
105-5	0.65	1.37	1.18	2.08	−2.3	−29.0
105-6	0.75	1.55	1.95	2.20	−2.4	−30.1
105-7	2.20	3.05	1.18	1.93	−3.3	−37.2
105-8	0.58	1.35	1.22	2.08	−2.5	−30.0
105-9	0.63	1.37	1.36	2.08	−1.9	−25.7
105-10	0.78	1.58	1.61	2.20	−2.1	−27.5
105-11	0.89	1.77	1.83	2.38	−2.2	−28.3
105-12	1.05	2.13	1.92	2.55	−2.6	−30.4
105-13	1.26	2.42	2.10	2.60	−2.7	−31.6
105-14	1.07	2.53	1.91	2.95	−3.0	−35.2
105-15	0.93	2.10	2.53	2.40	−2.7	−31.6
105-16	1.70	3.46	1.56	2.61	−3.2	−38.6
105-17	1.39	1.89	2.10	1.35	−3.7	−40.9
105-18	1.85	3.01	1.71	1.70	−4.1	−42.5
105-19	1.11	2.27	1.36	3.65	−2.9	−33.7
135-1	2.15	2.20	1.65	1.32	−3.9	−39.7
135-2	1.24	2.31	1.72	2.12	−3.0	−35.2
135-3	1.04	1.91	1.57	2.28	−2.9	−32.6
135-4	1.16	1.72	1.34	1.68	−3.5	−37.3
135-5	0.68	1.46	1.27	2.12	−2.3	−28.2
135-6	0.83	1.49	1.25	1.92	−2.6	−30.5
135-7	0.88	1.57	1.27	1.92	−2.7	−30.3
135-8	1.60	3.13	2.30	2.76	−3.0	−34.9
135-9	1.36	2.48	1.90	2.50	−2.7	−30.9
135-10	1.16	2.27	1.87	2.60	−2.7	−30.4
135-11	1.20	2.53	2.03	2.81	−2.8	−31.0
135-12	1.47	2.69	2.10	2.70	−2.5	−28.8
Seawater-1	0.38	1.13	0.91	3.63	−0.2	−5.2
Seawater-2	0.39	1.12	0.88	3.50	−0.2	−5.6
Saline water-1	0.55	1.18	1.26	2.23	−3.6	−32.0
Saline water-2	0.55	1.23	1.09	2.24	−2.4	−25.7
Saline water-3	0.45	1.06	0.84	3.54	−1.9	−21.1
Saline water-4	0.40	1.08	0.97	2.38	−1.4	−19.5
Saline water-5	0.32	1.09	0.98	3.63	−2.4	−24.0
Freshwater-1	0.10	0.01	0.01	0.01	−7.5	−53.4
Freshwater-2	0.14	0.04	0.02	0.12	−8.0	−57.8
Freshwater-3	0.21	0.04	0.05	0.10	−8.0	−57.2
Freshwater-4	0.08	0	0	0.01	−8.3	−59.0
River water	0.14	0.03	0.01	0.04	−7.1	−54.0

Such fluctuations of chemical concentrations suggest that multiple sources and hydrochemical processes act to generate the composition of the mine water.

Compared to the seepage water, the seawater and saline groundwater had similar pH (Avg. 7.33, SD 0.21), but decreased EC (Avg. 4.60×10^4 μS cm^{-1}, SD 3.66×10^3 μS cm^{-1}), Cl$^-$ concentration (Avg. 1.76×10^4 mg L^{-1}, SD 1.94×10^3 mg L^{-1}), Na$^+$ concentration (Avg. 9.89×10^3 mg L^{-1}, SD 1.44×10^3 mg L^{-1}), and TDS (Avg. 3.19×10^4 mg L^{-1}, SD 3.64×10^3 mg L^{-1}). As to the

Table 2 Chemical composition of water samples collected in July 2011

Sample	pH	EC (μS/cm) $\times 10^4$	TDS (mg/L) $\times 10^4$	Cl$^-$ (mg/L) $\times 10^4$	SO$_4^{2-}$ (mg/L) $\times 10^3$	HCO$_3^-$ (mg/L) $\times 10^2$
S105-01	7.23	3.92	3.32	1.83	2.47	2.26
S105-02	7.21	4.03	3.44	1.90	2.48	2.42
S105-06	7.37	4.08	3.41	1.90	2.39	2.54
S105-07	7.03	5.82	5.69	3.29	3.55	2.62
S105-10	7.25	4.27	3.60	2.00	2.71	2.43
S105-12	7.2	4.97	4.40	2.48	3.10	2.87
S105-13	7.19	4.88	4.35	2.42	3.17	2.93
S105-14	7.16	4.70	4.09	2.29	3.05	2.95
S105-16	7.13	6.61	6.86	3.96	4.61	2.42
S105-17	7.45	4.72	4.00	2.26	2.72	2.70
S135-03	7.14	4.67	4.09	2.27	2.88	2.39
S135-04	7.52	4.38	3.76	2.08	2.69	2.43
S135-07	7.52	4.31	3.79	2.12	2.57	2.48
S135-08	7.58	4.25	3.72	2.06	2.50	2.54
S135-09	7.2	5.44	5.12	2.85	3.67	3.22
S135-11	7.47	4.73	4.22	2.32	3.07	2.77
S135-12	7.39	4.88	4.35	2.43	3.15	2.90
S135-13	7.28	5.11	4.67	2.61	3.22	2.90

Sample	Ca^{2+} (mg/L) $\times 10^3$	Mg^{2+} (mg/L) $\times 10^3$	Na$^+$ (mg/L) $\times 10^4$	K$^+$ (mg/L) $\times 10^2$	δ^{18}O (‰)	δ^2H (‰)
S105-01	0.47	1.16	1.03	2.55	−1.7	−14.6
S105-02	0.52	1.19	1.08	2.48	−1.8	−8.7
S105-06	0.56	1.14	1.05	2.35	−1.9	−12.0
S105-07	1.68	2.25	1.61	1.85	−2.9	−21.6
S105-10	0.59	1.30	1.08	2.48	−1.5	−10.0
S105-12	0.76	1.53	1.33	2.53	−1.9	−8.0
S105-13	0.80	1.51	1.33	2.38	−2.0	−7.9
S105-14	0.60	1.33	1.25	2.43	−1.9	−7.2
S105-16	1.38	2.81	1.96	3.08	−2.7	−16.7
S105-17	1.00	1.47	1.18	1.60	−2.6	−13.8
S135-03	0.74	1.49	1.26	2.33	−2.1	−13.7
S135-04	0.65	1.28	1.17	2.53	−2.0	−11.3
S135-07	0.78	1.32	1.16	2.25	−2.4	−14.6
S135-08	0.79	1.29	1.16	2.13	−2.6	−17.7
S135-09	0.90	1.82	1.57	2.55	−2.3	−15.0
S135-11	0.72	1.44	1.32	2.55	−2.0	−9.9
S135-12	0.69	1.45	1.34	2.53	−2.0	−8.9
S135-13	0.88	1.59	1.43	2.55	−1.9	−12.4

freshwater and river water samples, it revealed much lower EC (Avg. 1.63×10^3 μS cm^{-1}, SD 1.17×10^3 μS cm^{-1}), TDS (Avg. 1.10×10^3 mg L^{-1}, SD 6.99×10^2 mg L^{-1}), concentrations of Cl$^-$ (Avg. 2.79×10^3 mg L^{-1}, SD 3.15×10^3 mg L^{-1}) and other cations and anions.

In contrast to the above results, the second round of hydrochemical analysis of the seepage water showed that many water quality parameters, such as the concentrations

of major ions, values of TDS, and EC experienced some changes under the influence of underground mining (Table 2). Of these water quality parameters, the most interesting were the TDS (Avg. 4.27×10^4 mg L^{-1}, SD 8.85×10^3 mg L^{-1}), Cl$^-$ concentrations (Avg. 2.39×10^4 mg L^{-1}, SD 5.32×10^3 mg L^{-1}), and Na$^+$ concentrations (Avg. 1.29×10^4 mg L^{-1}, SD 2.35×10^3 mg L^{-1}), which were greatly decreased compared to the measurement

in 2006 (Table 1). The increased pH (Avg. 7.30, SD 0.16) illustrated that the water sources of examined mine water experienced a certain degree of changes in the past five years of underground mining.

Water isotopes

The isotope ratios exhibit a broad range of values (Tables 1, 2). In the first round of measurement (July 2006), the $\delta^{18}O$ and $\delta^{2}H$ of seepage water varied from −4.1 to −1.8 ‰ and from −42.5 to −25.4 ‰, respectively. The most depleted sample is the 105-18 sample, which was collected at the cross drift of the filling shaft of the −105 m sublevel. The most enriched sample is the 105-1 sample, which was collected at the northeast strike drift of the −105 m sublevel. However, the isotopic measurements did not show a significant vertical variation between the −105 m sublevel and the−135 m sublevel. Compared to the seepage water, the seawater exhibited higher isotope ratios, i.e., the average value reached −0.2 ‰ for $\delta^{18}O$ and −5.4 ‰ for $\delta^{2}H$. In addition, the isotope ratios of freshwater exhibit uniform values covering about −8.0 ‰ for $\delta^{18}O$ and −-56.9 ‰ for $\delta^{2}H$. For the saline groundwater, the $\delta^{18}O$ were in the range of −1.4 to −3.6 ‰ and the $\delta^{2}H$ varied from −19.5 to −32.0 ‰. These isotope ratios indicated that the isotopic compositions were influenced by different water sources and hydraulic processes in the study area.

In contrast to the measurement results in 2006, the second round of measurement exhibited elevated isotope ratios after 5 years of mining. Values of $\delta^{18}O$ and $\delta^{2}H$ ranged from −1.5 to −2.9 ‰ and from −7.2 to −21.6 ‰, respectively (Table 2). These variations might attribute to the impacts of underground mining, which was presented in following Discussion section.

Discussion

Mine water geochemistry

As mentioned in the "Results" section, the hydrochemical composition of the seawater ranked the most stable, followed by the freshwater, the saline groundwater and the seepage water (Table 1). The seepage water revealed diverse chemistry and the quality parameters varied over a wide range in different sampling sites and different stages of exploitation. The piper diagram was used for water quality analysis (Piper 1944; Gammons et al. 2013). On the whole, the seepage water had mixed major-ion chemistry (Fig. 3), dominated by Na–Cl hydrochemical species. In addition, the sample of Freshwater-3 showed higher EC, TDS, and Cl⁻ concentration than other freshwater samples.
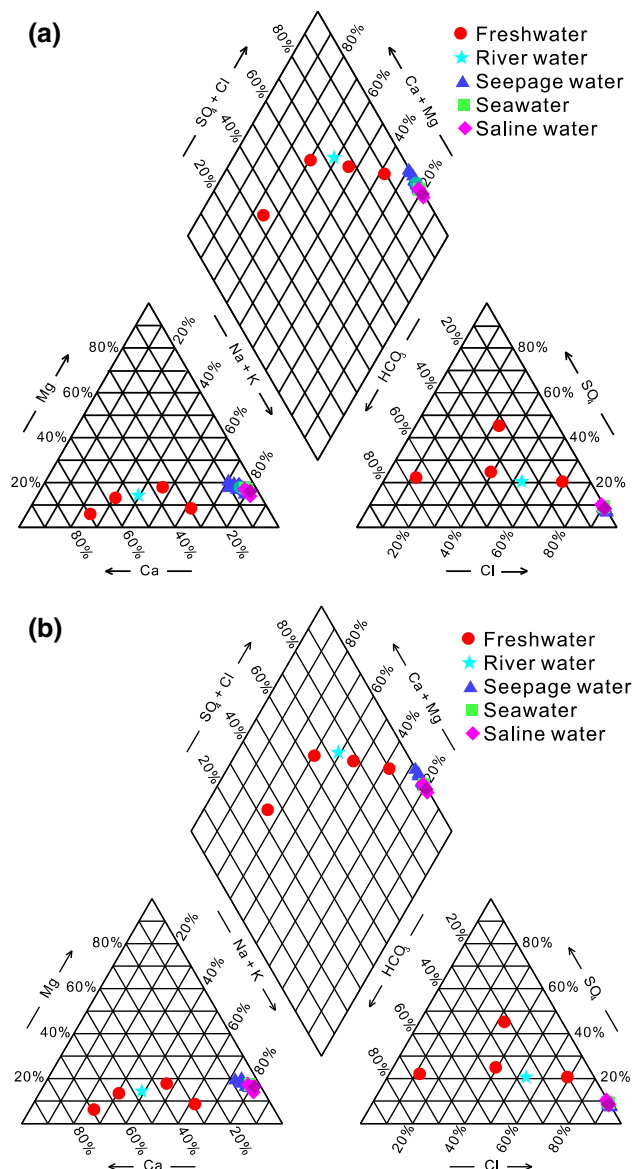

Fig. 3 Piper diagrams for water samples collected in 2006 (**a**) and 2011 (**b**). Data for seawater, saline water, freshwater, and river water, brine, and atmospheric precipitation were assured invariable from 2006 to 2011

The sampling depth of the water sample is only 4 m under the ground surface. Thus, the sampled well water might be mixed a certain amount of saline water because of saline intrusion (Ma et al. 2007). Even so, this water sample could be categorized into freshwater because their chemical parameters were still significantly smaller than those of the saline water and seawater samples.

Different sources of mine water

Overall, there were three basic types of water contributed to the mine water, i.e., seawater, brine, and Quaternary water.

The Quaternary water included the saline groundwater and freshwater. The former provided the far-field recharge of the mine water, while the latter supplied the near-field recharge of mine water. The ultimate origin of Quaternary water is atmospheric precipitation. Besides the seawater and brine, the atmospheric precipitation was regarded as a basic source of mine water for the convenience of discussion in this study. Given this understanding, the regional chemical and isotopic results of atmospheric precipitation and brine in the mine area were applied to study the formation of mine water. For the regional atmospheric precipitation, the values of TDS, $\delta^{18}O$, and $\delta^{2}H$ are 100 mg L^{-1}, -10.1, and -75.2 ‰, respectively. For the brine, the values of TDS, $\delta^{18}O$, and $\delta^{2}H$ are 9.26×10^4 mg L^{-1}, -2.4, and -38.1 ‰, respectively (Sun et al. 2002).

Stable H and O isotope ratios of all water samples measured in 2006, including the regional precipitation and brine water, were plotted in Fig. 4. All samples are located on the right flank of the global meteoric water line (GMWL) (Craig 1961). The $\delta^{18}O$ and $\delta^{2}H$ of seawater samples show comparatively large values because of the intense evaporation on the surface of the sea. The $\delta^{18}O$ of the brine groundwater deviates from the GMWL far to the right and indicated it is originated from evaporated modern seawater (Ma et al. 2007). The freshwater samples are located on the lower-right of the GMWL. It suggests that the shallow fresh groundwater is originated from precipitation and experienced evaporation for a long time (Ma et al. 2007). For the saline groundwater and seepage water samples, they are distributed between the precipitation and seawater/brine, resulting from mixing of freshwater and seawater or/and brine. The difference is that the saline groundwater samples are distributed close to the precipitation-seawater line. This indicates that the saline groundwater is the mixture of precipitation and seawater and undergoes evaporation (Ma et al. 2007). In contrast, the
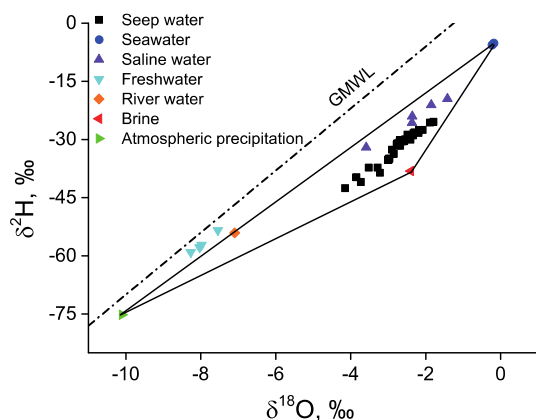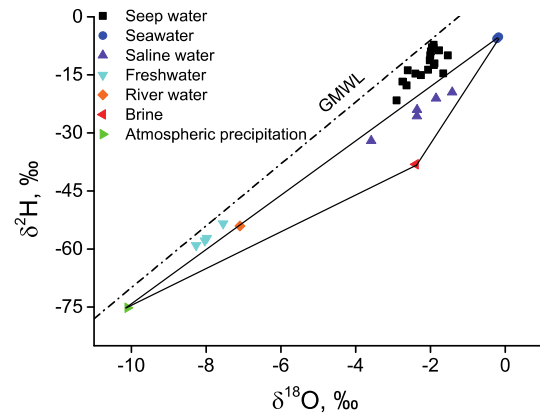

Fig. 5 Isotopic ratios for water samples collected in July 2011. Data for seawater, saline water, freshwater, and river water, brine, and atmospheric precipitation were assured invariable from 2006 to 2011 (modified from Craig 1961)

seepage water samples are distributed close to the seawater-brine line, indicating that they are mainly the mixture of seawater and brine. Furthermore, these seepage water samples are close to the brine side in Fig. 4. It can be deduced that the seepage water is mainly composed of brine, and then followed by seawater and atmospheric precipitation.

Suppose the $\delta^{2}H$ and $\delta^{18}O$ of the seawater, precipitation, saline groundwater, and brine in the study area are constant in a relatively short period of mining activities. The $\delta^{18}O$ and $\delta^{2}H$ of seepage water that measured in 2011 were plotted in Fig. 5 for further study of their changes. Compared to Fig. 4, great changes have taken place in the distribution of the seepage water samples. All seepage water samples are distributed on the left flank of the precipitation-seawater line and deviated far to the brine side, indicating that the seepage system experienced great changes and the proportion of seawater significantly increased in the mine discharge after five years of exploitation.

Determination of the mixing proportions

On the basis of the above analysis, the mine water is actually a mixture of seawater, brine, and atmospheric precipitation, which discharge into the mine tunnels through different seepage pathways. In the mine area, the seawater, saline groundwater, brine, and seepage water are almost Na–Cl hydrochemical species. Only a few seepage water samples are Cl–Na·Mg hydrochemical species. Therefore, no chemical precipitations were produced in the mixing process. In this case, a ternary hybrid model that composed of seawater, brine, and atmospheric precipitation was established to evaluate their possible proportions in the mine discharge (Qin and Ma 2005; Liu et al. 2007). In calculating the mixture ratios, the accuracy and reliability

Fig. 4 Isotopic ratios for water samples collected in July 2006 (modified from Craig 1961)

of the results depends on the representativeness of the selected parameter. In this study, positive linear relationships occurred between the TDS and Cl^- concentration in all water samples, and the $\delta^{18}O$ and TDS showed high degrees of stability. Thus, the parameters of $\delta^{18}O$ and TDS were chosen for the subsequent quantitative calculation.

In this case, the following parameters can be served as known quantities:

Seawater: TDS $= 2.97 \times 10^4$ mg L^{-1}, $\delta^{18}O = -0.2$ ‰, Brine: TDS $= 9.26 \times 10^4$ mg L^{-1}, $\delta^{18}O = -2.4$ ‰, Atmospheric precipitation: TDS $= 100$ mg L^{-1}, $\delta^{18}O = -10.1$ ‰.

Assume the TDS and $\delta^{18}O$ of a seepage point is measured as m and $-n$‰, and the composition of seawater, brine, and atmospheric precipitation count for $a\%$, $b\%$ and $c\%$ respectively. Thus obtaining:

$$\begin{cases} 2.97 \cdot a\% + 9.26 \cdot b\% + 0.01 \cdot c\% = m \cdot 100\% \\ 0.2 \cdot a\% + 2.4 \cdot b\% + 10.1 \cdot c\% = n \cdot 100\% \\ a\% + b\% + c\% = 100\% \end{cases} \quad (3)$$

Substituting the values of TDS and $\delta^{18}O$ measured in Tables 1 and 2 for each seepage point into Eq. (1), the proportions of seawater, brine, and atmospheric precipitation for each seepage point can be solved. As illustrated in Figs. 6 and 7, the mixing proportions of seepage water samples showed great differences. Both the high brine content sample (105-16) and the high seawater content sample (105-1) occurred in the −105 m sublevel. Moreover, significant vertical variation in the mixing proportions of the seawater and brine were revealed in the calculation results. Overall, most of the water samples showed higher proportions of seawater but lower proportions of brine in the −105 m sublevel than those in the −135 m sublevel. Furthermore, the mixing proportions of the seepage water underwent great changes in the next 5 years. As show in Fig. 8, the proportions of seawater increased substantially, while the proportions of the brine decreased appreciably in all comparable water samples. The fundamental reason for the changes lies in the persistent mining disturbance.

However, it is impossible to calculate accurate proportions of the three types of water for the entire mine because these water samples account for only a small fraction of water discharge. As the majority of the seepage points had similar discharge characteristics, the calculation of average mixing proportions based on the tested samples may be beneficial to acquire comprehensive knowledge on the water discharge characters of the mine tunnels. Under such situations, the results of the calculation show that the proportions of seawater, brine and precipitation discharge were about 38.5, 46, and 15.5 % for the entire mine in 2006, which changed to 59.6, 27, and 13.4 % in 2011 (Figs. 6, 7). Therefore, it can be seen
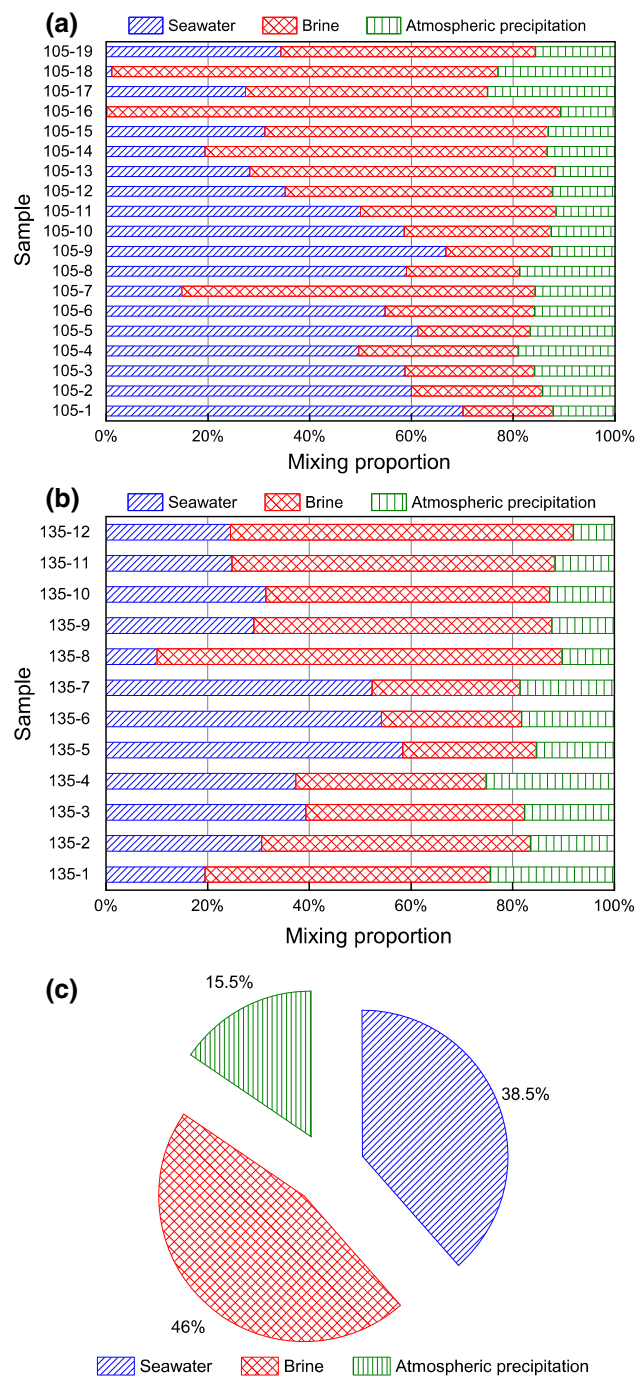

Fig. 6 Mixing proportions of seawater, brine, and atmospheric precipitation in July 2006. **a** Water samples collected in the −105 m sublevel of the mine tunnels, **b** water samples collected in the −135 m sublevel of the mine tunnels, and **c** average mixing proportions for the entire mine

that proportion of seawater increased 21.1 % and the proportion of brine decreased 19 %.

The main reason for the increase of seawater in the mine water can be attributed to the mining influence. Although the cut-and-fill mining method that applied in the Xinli mine
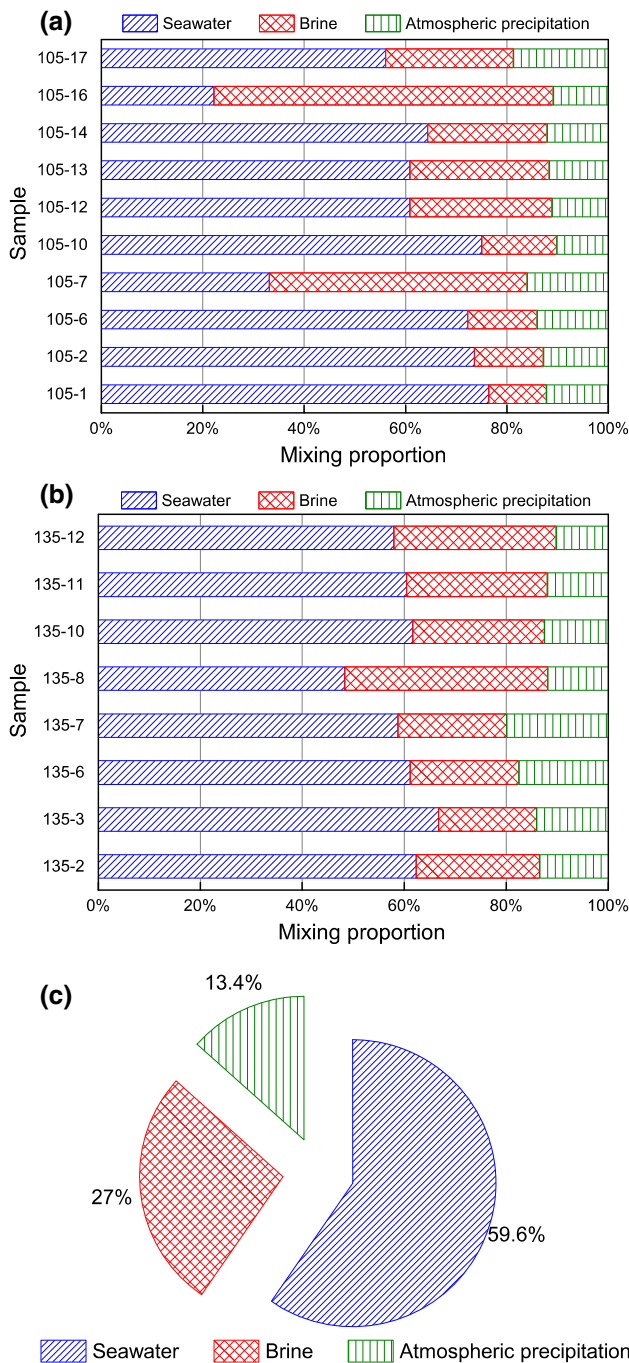
(a)

(b)

(c)

Fig. 7 Mixing proportions of seawater, brine, and atmospheric precipitation in July 2011. **a** Water samples collected in the −105 m sublevel of the mine tunnels, **b** water samples collected in the −135 m sublevel of the mine tunnels, and **c** average mixing proportions for the entire mine

could control ground pressure and prevent superincumbent ground movement and deformation from occurring (Bell et al. 2000; Swift and Reddish 2002), this mining method has been proved that large-scale rock mass movement and deformation cannot be avoided absolutely because the effects of large-scale stress adjustment and redistribution, hysteretic backfill,
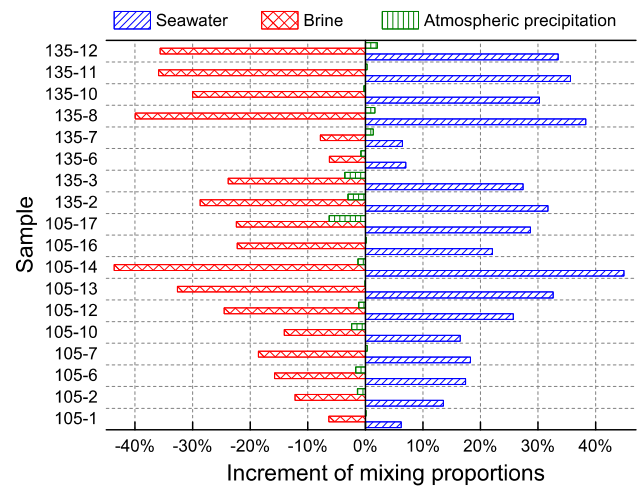

Fig. 8 Variation of mixing proportions for corresponding water samples (2006–2011)

low strength of filling body, unfilled void space, as well as repeated mining activities may concurrently arise during underground mining (Li et al. 2004; Zhao et al. 2008, 2013). The surrounding rock mass deformation and failure may not only enhance the strata hydraulic conductivity but also generate watercourse and water inrush in the mine. The Xinli mine is facing similar problems although it is still in the initial stages. Despite the lack of monitoring data in the ground surface of the mine area, the considerable increase in the proportion of seawater indicates that the underground mining activities significantly enhanced the hydraulic conductivity of the surrounding rocks, which could provide access to water inflow into the mine tunnels in the process of mining.

Conclusions

In the Xinli subsea mine, the overlying Quaternary aquifer and seawater pose great threats to the underground mining operations. Chemical analyses were used to study the relationships between the various waters and the processes affecting their composition in the study area.

The seepage water in the mine tunnels had higher concentrations of some elements, TDS, and EC compared to the seawater and saline groundwater. However, the concentrations of these analyses measured in 2006 decreased in 2011. In addition, the isotope composition of the waters indicated the seepage samples were more isotopically enriched than modern seawater but less than brine. Water analyses indicated the mine discharge was a mixture of the seawater, brine, and atmospheric precipitation. The proportions of the three different sources were calculated on the basis of hydrochemical and isotopic analyses. It revealed that almost all seepage water had higher proportions of seawater but lower proportions of brine in the

−105 m sublevel than that in the −135 m sublevel. Overall, the average proportions of the seawater, brine and atmospheric precipitation discharge were about 38.5, 46, and 15.5 %, respectively for the entire mine in 2006. However, the proportion of the seawater increased 21.1 % and the brine decreased 19 % after 5 years of exploitation. It was inferred that the surrounding rock mass underwent a certain extent of deformation and the expansion of water-conducting fractured zone enhanced the hydraulic conductivity of the surrounding rock mass.

Although the long-term application of groundwater geochemistry have helped understanding some aspects of the origin of mine water of the Xinli mine tunnels, additional study involving installation of monitoring wells and displacement sensors could help in raising awareness of the hydraulic connections and changes of the rock mass structures.

References

Aston TRC, Whittaker BN (1985) Undersea longwall mining subsidence with special reference to geological and water occurrence criteria in the North-East of England coalfield. Min Sci Technol 2(2):105–130. doi:10.1016/S0167-9031(85)90335-4

Bell FG, Stacey TR, Genske DD (2000) Mining subsidence and its effect on the environment: some differing examples. Environ Geol 40(1/2):135–152. doi:10.1007/s002540000140

Birkle P, Merkel B, Portugal E et al (2001) The origin of reservoir fluids in the geothermal field of Los Azufres, Mexico—isotopical and hydrological indications. Appl Geochem 16(14):1595–1610. doi:10.1016/S0883-2927(01)00031-2

Castilla JC, Nealler E (1978) Marine environmental impact due to mining activities of El Salvador copper mine, Chile. Mar Pollut Bull 9(3):67–70. doi:10.1016/0025-326X(78)90451-4

Chapman EC, Capo RC, Stewart BW et al (2013) Strontium isotope quantification of siderite, brine and acid mine drainage contributions to abandoned gas well discharges in the Appalachian Plateau. Appl Geochem 31:109–118. doi:10.1016/j.apgeochem.2012.12.011

Craig H (1961) Isotope variations in meteoric waters. Science 133:1702–1703

Epstein S, Mayeda T (1953) Variation of O18 content of water from natural sources. Geochim Cosmochim Ac 4:213–224. doi:10.1016/0016-7037(53)90051-9

Gammons CH, Brown A, Poulson SR et al (2013) Using stable isotopes (S, O) of sulfate to track local contamination of the Madison karst aquifer, Montana, from abandoned coal mine drainage. Appl Geochem 31:228–238. doi:10.1016/j.apgeochem.2013.01.008

Garing C, Luquot L, Pezard PA et al (2013) Geochemical investigations of saltwater intrusion into the coastal carbonate aquifer of Mallorca, Spain. Appl Geochem 39:1–10. doi:10.1016/j.apgeochem.2013.09.011

Garritty P (1983) Water flow into undersea mine workings. Geotech Geol Eng 1(3):237–251

Ghosh AK, Mukhopadhyay R (2000) Mineral wealth of the ocean. A.A. Balkema, Rotterdam

Glasby GP (2000) Lessons learned from deep-sea mining. Science 289(5479):551–553. doi:10.1126/science.289.5479.551

Glasby GP (2002) Deep seabed mining: past failures and future prospects. Mar Georesour Geotec 20(2):161–176. doi:10.1080/03608860290051859

González-Partida E, Carrillo-Chávez A, Levresse G et al (2005) Hydro-geochemical and isotopic fluid evolution of the Los Azufres geothermal field, Central Mexico. Appl Geochem 20(1):23–39. doi:10.1016/j.apgeochem.2004.07.006

Halfar J, Fujita RM (2002) Precautionary management of deep-sea mining. Mar Policy 26(2):103–106. doi:10.1016/S0308-597X(01)00041-0

Han D, Kohfahl C, Song X et al (2011) Geochemical and isotopic evidence for palaeo-seawater intrusion into the south coast aquifer of Laizhou Bay, China. Appl Geochem 26(5):863–883. doi:10.1016/j.apgeochem.2011.02.007

Jewett SC, Feder HM, Blanchard A (1999) Assessment of the benthic environment following offshore placer gold mining in the northeastern Bering Sea. Mar Environ Res 48(2):91–122. doi:10.1016/S0141-1136(99)00034-3

Katherine WD, Eileen P (2009) Investigating hydraulic connections and the origin of water in a mine tunnel using stable isotopes and hydrographs. Appl Geochem 24(12):2266–2282. doi:10.1016/j.apgeochem.2009.09.015

Li X, Wang SJ, Liu TY et al (2004) Engineering geology, ground surface movement and fissures induced by underground mining in the Jinchuan Nickel Mine. Eng Geol 76(1–2):93–107. doi:10.1016/j.enggeo.2004.06.008

Li X, Li D, Liu Z et al (2013) Determination of the minimum thickness of crown pillar for safe exploitation of a subsea gold mine based on numerical modelling. In J Rock Mech Min Sci 57:42–56. doi:10.1016/j.ijrmms.2012.08.005

Liu C, Peng B, Qin J (2007) Geological analysis and numerical modeling of mine discharges for the Sanshandao gold mine in Shandong, China: 1. Geological Analysis. Mine Water Environ 26(3):160–165. doi:10.1007/s10230-007-0004-6

Ma F, Yang YS, Yuan R et al (2007) Study of shallow groundwater quality evolution under saline intrusion with environmental isotopes and geochemistry. Environ Geol 51(6):1009–1017. doi:10.1007/s00254-006-0370-6

Mahmoud K, Corinne LGLS, Joël L et al (2013) Origin of groundwater salinity (current seawater vs. saline deep water) in a coastal karst aquifer based on Sr and Cl isotopes. Case study of the La Clape massif (southern France). Appl Geochem 37:212–227. doi:10.1016/j.apgeochem.2013.07.006

Migaszewski Z, Gałuszka A, Hałas S et al (2009) Chemical and isotopic variations in the Wiśniówka Mała mine pit water, Holy Cross Mountains (south-central Poland). Environ Geol 57(1):29–40. doi:10.1007/s00254-008-1279-z

Park HY, Jang K, Ju JW et al (2012) Hydrogeological characterization of seawater intrusion in tidally-forced coastal fractured bedrock aquifer. J Hydrol 446–447:77–89. doi:10.1016/j.jhydrol.2012.04.033

Parker SR, Gammons CH, Garrett Smith M et al (2012) Behavior of stable isotopes of dissolved oxygen, dissolved inorganic carbon and nitrate in groundwater at a former wood treatment facility containing hydrocarbon contamination. Appl Geochem 27(6):1101–1110. doi:10.1016/j.apgeochem.2012.02.035

Pellicori DA, Gammons CH, Poulson SR (2005) Geochemistry and stable isotope composition of the Berkeley pit lake and surrounding mine waters, Butte, Montana. Appl Geochem 20(11):2116–2137. doi:10.1016/j.apgeochem.2005.07.010

Piper AM (1944) A graphical procedure in the geochemical interpretation of water analysis. Trans Am Geophys Union 25:914–928

Qin H, Ma ZY (2005) Hydrogeochemistry. Geological Publishing House, Beijing, pp 133–135

Révész K, Coplen TB (2007) Determination of the $\delta(^2H/^1H)$ of water: RSIL lab code 1574. In: Révész K, Coplen TB (eds) Methods of the Reston Stable Isotope Laboratory. US Geological Survey, Techniques and Methods, Techniques and Methods (Book 10, sec. C, Chapter 1), Reston

Révész K, Coplen TB (2008) Determination of the $\delta(^{18}O/^{16}O)$ of water: RSIL lab code 489. In: Révész K, Coplen TB (eds) Methods of the Reston Stable Isotope Laboratory. US Geological Survey, Techniques and Methods, Techniques and Methods, (Book 10, Sect. C, Chapter 2), Reston

Sui WH, Xu ZM (2013) Risk assessment for coal mining under sea area. In: Huang Y, Wu FQ, Shi ZM, Ye B (eds) New Frontiers in Engineering Geology and the Environment. Springer-Verlag, Berlin, pp 199–202. doi:10.1007/978-3-642-31671-5_35

Sun Z, Zhu Z, Li W (2002) Geological exploration report of Xinli gold mine. Laizhou Geological and Mineral Exploration Institute, Laizhou

Swift GM, Reddish DJ (2002) Stability problems associated with an abandoned ironstone mine. B Eng Geol Environ 61:227–239. doi:10.1007/s10064-001-0147-9

Wang WX, Hu W, Liang YK (2013) Experimental investigation for water flowing fractured zone due to coal mining under sea area. In: Huang Y, Wu FQ, Shi ZM, Ye B (eds) New Frontiers in Engineering Geology and the Environment. Springer-Verlag, Berlin, pp 207–209. doi:10.1007/978-3-642-31671-5_37

Zhao HJ, Ma FS, Li GQ et al (2008) Analysis and mechanism of ground movement, deformation and fracture induced by underground backfill mining. Chin J Geotech Eng 30(5):670–676

Zhao HJ, Ma FS, Zhang YM et al (2013) Monitoring and mechanisms of ground deformation and ground fissures induced by cut-and-fill mining in the Jinchuan Mine 2, China. Environ Earth Sci 68(7):1903–1911. doi:10.1007/s12665-012-1877-7